

# Podolsky quantum electrodynamics for strongly coupled Dirac fermions in (2+1)D

Carlos A. P. C. Junior,<sup>1,\*</sup> Leandro O. Nascimento,<sup>2,3,†</sup> and Van Sérgio Alves<sup>1,2,‡</sup>

<sup>1</sup>*Programa de Pós Graduação em Física, Universidade Federal do Pará, 66075-110 Belém, Pará, Brazil*

<sup>2</sup>*Faculdade de Física, Universidade Federal do Pará, 66075-110 Belém, Pará, Brazil*

<sup>3</sup>*Programa de Pós Graduação em Física, Universidade Federal de Campina Grande, 58429-900 Campina Grande, Paraíba, Brazil*

(Dated: October 23, 2025)

We investigate Podolsky quantum electrodynamics (POQED), a higher-derivative extension of QED in (3+1)D, and perform its dimensional reduction to (2+1)D by confining the Dirac current to a plane while allowing the gauge field to propagate out of the plane. The resulting model, which we call Pseudo Generalized QED (PGQED), is minimally coupled to massless Dirac fermions. In the strong-coupling regime, we show that a dynamical mass is generated through approximate solutions of the Schwinger-Dyson equation, leading to chiral symmetry breaking and modifications of the fermion dispersion relation. We derive an analytic critical coupling  $\alpha_c(\mu)$  and flavors critical number  $N_c(\mu)$ , dependent on the Podolsky parameter  $\mu$  and the ultraviolet cutoff  $\Lambda$ . These analytical results are found to be consistent with the numerical analysis. Finally, we discuss connections to graphene, estimating a range for  $\mu$  in the ultrarelativistic limit.

## I. INTRODUCTION

One of the most important features of low-dimensional quantum field theories is the possibility of chiral symmetry breaking in (2+1)D for both QED and four-fermion interacting theories (such as the Nambu-Jona-Lasinio model) [1, 2]. The order parameter for chiral symmetry breaking is the so-called dynamically generated mass for the fermion, usually calculated by using the Schwinger-Dyson equations. The interest in this topic has emerged first as a simplified framework for studying confinement in quantum chromodynamics in the strongly correlated limit [3]. Thereafter, due to the experimental realization of graphene [4] and the observation of Dirac cones in (2+1)D, these effective models have also been applied in the physics of two-dimensional materials [2, 5, 6]. In this case, the main idea is to derive a quantum phase transition from a previously massless spectrum to an electronic band with a gap, which has direct consequences for transport properties of the material [5].

When considering the physics of two-dimensional materials, Pseudo quantum electrodynamics (PQED) [7] has provided several results that have been compared to experimental findings [8–13]. PQED is obtained from a dimensional reduction of QED in (3+1)D, where the main physical assumption in PQED is to confine the dynamics of the matter current to a spatial plane. Furthermore, the dimensional reduction of QED with a massive photon has also been explored in Ref. [14], where it is shown an effective gauge field theory that describes the Yukawa interaction in (2+1)D. Emergent gauge fields, therefore, have been shown to be an important tool for calculating interacting effects among either confined electrons or

quasiparticles in two-dimensional materials. Within the many-body physics, the role of the Yukawa potential is to modify the Coulomb potential such that the charge screening becomes relevant for the physics of the system. This has also been discussed by using ultracold atoms in optical lattices [14].

The GQED, proposed by Boris Podolsky in 1942, is a model that introduces a higher-order derivative term into the standard quantum electrodynamics (QED), yielding a characteristic parameter  $a$  with units of inverse of mass, called the Podolsky parameter [15]. Whenever this parameter vanishes, one recovers Maxwell's theory. This GQED preserves both Lorentz and gauge symmetries while describing a massive mode for the gauge field, beyond the standard massless photon [16]. Furthermore, GQED provides a finite potential for a point-like particle at short distances, unlike electrons within conventional QED [15]. Hence, one expects a better UV behavior of the model in comparison to QED, which may have consequences for renormalizability of the theory. The dimensional reduction of GQED has not been considered until now. In Ref. [17] a similar model has been considered within classical field theory.

In this work, we perform a dimensional reduction in GQED and obtain a reduced model which we call as PGQED, fully defined in (2+1)D. Within the strongly correlated limit, we calculate a dynamically generated mass to an initially massless Dirac electron. Similarly to PQED, we consider that the matter current is confined to move only in a spatial plane (for example  $j_z = 0$ ), such as electrons in a monolayer of graphene, while the gauge field is free to propagate in (3+1)D. This hybrid situation has been discussed in Ref. [7] in the context of QED. For PGQED, the static potential among electrons reads  $V(r) \propto (1 - e^{-r/a})/r$ , recovering the Coulomb interaction when  $a \rightarrow 0$ . Note that this kind of interaction allows us to approximate the static electromagnetic interaction by a local four-fermion action, given by  $\propto \rho_0^2/a$  at short distances  $r \ll a$ , where  $\rho_0 = \psi\gamma_0\psi$  is the charge

---

\* carlos.chaves.junior@ufpa.br

† lon@ufpa.br

‡ vansergji@ufpa.br

density of the Dirac field  $\psi$ . For a full description of the interaction, as will become clear later, we shall consider a gauge field theory with a pseudo-differential operator.

The dynamical mass generation implies a chiral symmetry breaking in (2+1)D whenever we consider Dirac fermions in the four-rank representation of Dirac matrices [1, 3]. Hence, for strong interactions, we consider a suitable set of approximations to solve the Schwinger-Dyson equations. In particular, we find nontrivial solutions for the mass function  $\Sigma(p)$  of the full electron propagator, using both the rainbow-quenched and rainbow-unquenched approximations. In general, when  $\Sigma(p) \neq 0$ , we have a dynamically generated mass. For  $\Sigma(p \rightarrow 0) = M$ , which is a quite simplistic solution, it follows that  $M$  is the pole of the full fermion propagator, therefore, it would be the dynamical mass of the electron. Furthermore, we show that  $M$  corresponds to a small fraction of the UV cutoff  $\Lambda$ , which plays an important role in our model. This parameter can be related to the lattice constant  $a_L \approx 10^{-10}$  m of graphene, hence  $\Lambda \approx 1$  eV which works as an upper energy limit for our Dirac cones [18]. Indeed, for energies above this value one would observe corrections to the Dirac cones and, therefore, the Dirac approximation for electrons in graphene becomes less reliable [5]. Here, we consider  $\Lambda$  to be a large energy value. We also consider a full Lorentz invariant matter field, which simplifies the calculation of the electron self-energy. This can also be realized in graphene in the low-density limit of charge carriers, as discussed in Ref. [18]. Improved approximations show that there exist a critical coupling constant  $\alpha_c$  and a critical number of fermions  $N_c$  that separate the symmetry and broken phases. These parameters bound the values of the fine-structure constant  $\alpha \propto e^2/4\pi$  ( $\alpha > \alpha_c$ ) and the number of degrees of freedom  $N$  ( $N < N_c$ ). Finally, we also describe the relevance of the Podolsky parameter  $\mu = a^{-1}$  for the onset of this quantum phase transition.

The outline of this paper is following: In Sec. II, we derive our model and its Feynman rules. In Sec. III, we discuss the Schwinger-Dyson equation for our model. In Sec. IV and V, we calculate the mass function using a suitable set of approximations. In Sec. VI, we discuss our main results and their consequences. We also include one Appendix A where we show details about the dynamical mass generation and Appendix B where we show the numerical results for the mass function and the renormalization of the wavefunction of the electron.

## II. THE MODEL

In this section, we calculate the dimensional reduction of GQED from (3+1)D to (2+1)D [19]. This follows the same method applied for deriving PQED [7].

Firstly, let us define the Lagrangian of GQED, in Eu-

clidean space,

$$\mathcal{L}_{\text{GQED}} = \frac{1}{4} F_{\mu\nu} F^{\mu\nu} - \frac{a^2}{2} \partial_\nu F^{\mu\nu} \partial^\sigma F_{\mu\sigma} + \bar{\psi}(i\not{\partial} - m)\psi + e\bar{\psi}\gamma_\mu\psi A^\mu + \frac{\xi}{2}(\partial_\mu A^\mu)^2, \quad (1)$$

where  $A_\mu$  is a gauge field and  $F_{\mu\nu} = \partial_\mu A_\nu - \partial_\nu A_\mu$  is its strength tensor. The constant  $a$  is the Podolsky parameter and it multiplies a higher-order derivative term. We also include a gauge fixing term  $\xi$ . On the other hand,  $\psi$  is the Dirac field,  $m$  is its bare mass,  $e$  is the fundamental charge of electron, and  $\gamma_\mu$  are the Dirac matrices with  $\mu = 0, 1, 2, 3$ . We also consider  $c = \hbar = 1$  everywhere. The details regarding the dimensional reduction are shown in Appendix A. From these calculations, it follows that the reduced version of Eq. (1) is

$$\mathcal{L}_{\text{PGQED}} = \frac{1}{4} \tilde{F}_{\mu\nu} K_E[\square] \tilde{F}^{\mu\nu} + \bar{\psi}(i\not{\partial} - m)\psi + e\bar{\psi}\gamma_\mu\psi \tilde{A}^\mu + \frac{\xi}{2} \partial_\mu \tilde{A}^\mu K_E[\square] \partial_\nu \tilde{A}^\nu, \quad (2)$$

where  $\tilde{A}_\mu$  is fully defined in (2+1)D ( $\mu = 0, 1, 2$ ) and  $\tilde{F}_{\mu\nu} = \partial_\mu \tilde{A}_\nu - \partial_\nu \tilde{A}_\mu$  is its strength tensor, similarly as in Eq. (1). We call the model in Eq. (2) Pseudo generalized quantum electrodynamics (PGQED). A similar calculation has been discussed in Ref. [17], using a different kind of higher-order derivative term.

Furthermore, the pseudo-differential operator  $K_E[\square]$  reads

$$K_E[\square] = \frac{2(-\square + \mu^2)}{(-\square + \mu^2)(-\square)^{1/2} - (-\square)(-\square + \mu^2)^{1/2}}, \quad (3)$$

where we have defined a new constant  $\mu = 1/a$  with dimension of mass and  $\square$  is the standard d'Alembertian operator. This complicated kernel allows this model to reproduce the very same interaction of the model in Eq. (1), but for confined electrons in a plane.

Next, let us discuss the interaction between static charges. The dimensional reduction is defined in order to preserve the electron-electron interaction (See Appendix A). Hence, for consistency, we obtain the same potential of GQED in Eq. (1), namely,

$$V(r) = \frac{e^2}{4\pi r} (1 - e^{-r/a}). \quad (4)$$

For small distances  $r \ll a$ , the potential is finite and given by  $e^2/4\pi a$  at lowest-order approximation, which is a feature of GQED. For larger distances  $r \gg a$ , we obtain the Coulomb potential as in QED in (3+1)D. On the other hand, for intermediate values  $r \approx a$ , we have a Coulomb potential with a screened electric charge. In Fig. 1, we plot Eq. (4) using an artificial value for  $a$ . These results mostly concern the classical physics of GQED. From now on, we shall consider quantum effects of the dimensional reduction of GQED.

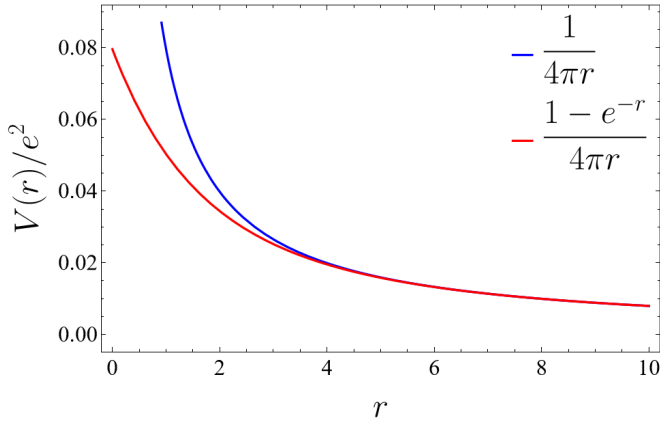


Figure 1. *The static potential of PGQED.* The red line represents the PGQED potential, given by Eq. (4), and is plotted for  $a = 1$ . The blue line represents the Coulomb potential of QED, obtained from Eq. (4) in the limit  $a \rightarrow \infty$ . Note that the PGQED potential is finite at the origin.

In the realm of quantum field theory, in particular for QED in (3+1)D, we need to deal with divergences when calculating quantum corrections to the Green functions of the model. It turns out that the better behavior for  $r \rightarrow 0$  of GQED implies, in general, a way to deal with these divergences. For our model, given by Eq. (2), we should also observe a better UV behavior when compared to PQED, which can be analyzed by calculating the Feynman rules of this action.

### A. The Feynman Rules

In this section, we derive the Feynman rules for PGQED in Eq. (2) at tree level. This is mandatory to apply the so-called Schwinger-Dyson equations for calculating the full Green functions of the model, which we shall discuss later. After a standard algebra, we obtain the bare gauge-field propagator, given by

$$\Delta_{\mu\nu}^0(p) = \left[ \frac{1}{2} \frac{1}{(p^2)^{1/2}} - \frac{1}{2} \frac{1}{(p^2 + \mu^2)^{1/2}} \right] \left[ \delta_{\mu\nu} - \frac{p_\mu p_\nu}{p^2} \right], \quad (5)$$

where we use the Landau gauge, i.e.,  $\xi \rightarrow +\infty$ . After integrating out the gauge field in Eq. (2), it is straightforward to conclude that static charges interact through the potential  $V(r)$  in Eq. (4), which is obtained from the Fourier transform of  $\Delta_{00}^0(p_0 = 0, \mathbf{p})$  [20]. Note that whether  $\mu \rightarrow \infty$  (and equivalently  $a \rightarrow 0$ ), we recover the PQED model as expected. Furthermore, in contrast to standard GQED, we can not conclude that this propagator in Eq. (5) describes either a massive or massless particle. Indeed, due to the square root in the gauge-field propagator, it does not have a pole and it needs a branch cut in order to become a single-valued function in the complex plane of  $p$ . Some important features of this propagator have been discussed in Ref. [17] at classical

level.

On the other hand, the bare fermion propagator reads

$$S_{0F} = \frac{1}{-\not{p} + m} \quad (6)$$

and the bare interaction vertex is given by

$$e\gamma^\mu, \quad (7)$$

where the Dirac matrices  $\gamma^\mu$  satisfy the Clifford algebra, namely,  $\{\gamma^\mu, \gamma^\nu\} = -2\delta^{\mu\nu}$ . From now on, let us assume that these matrices are written in a four-rank representation, which allows us to discuss the chiral symmetry breaking driven by a dynamically generated mass [1, 2]. From Eq. (6), we obtain, after a Wick rotation  $p_0 \equiv E \rightarrow iE$ , the standard Dirac energy  $E_\pm(\mathbf{p}) = \pm\sqrt{\mathbf{p}^2 + m^2}$ . The model is symmetric under chiral symmetries whenever  $m \rightarrow 0$ . Interestingly, for both QED and PQED, this symmetry may be broken due to quantum corrections for strongly correlated electrons. Here, we want to describe how  $\mu$  changes this effect. In order to do so, we shall define the Schwinger-Dyson equations for the full propagators.

### III. SCHWINGER-DYSON EQUATIONS FOR PGQED

A dynamically generated mass for the Dirac field, in this case, implies a breaking of the chiral symmetry. This, nevertheless, is usually a nonperturbative effect in quantum field theory. Here, we use the Schwinger-Dyson equations for PGQED in order to study this problem

These equations are a set of coupled nonlinear integral equations involving all of the corrected Green's functions of a given theory and, after solving them, provide us the whole physics described by the model [3, 21, 22].

Because we are interested in calculating the dynamically generated mass for the fermion, hence, it would be enough to calculate the full electron propagator. Therefore, let us consider only the full two-point functions for both the gauge and matter fields, which are coupled to the full three-point vertex interaction. Hence, we need the Schwinger-Dyson equations for the three relevant Green functions of this problem: one equation to the gauge-field propagator; an equation for the fermion propagator; and one equation for the vertex interaction [3]. In the case of the gauge-field propagator, we have

$$\Delta_{\mu\nu}^{-1}(p) = \Delta_{0\mu\nu}^{-1}(p) - \Pi_{\mu\nu}(p), \quad (8)$$

where  $\Delta_{\mu\nu}^{-1}(p)$  is the full gauge-field propagator with all of the radiative corrections. The first term on the rhs of Eq. (8) is the inverse of the gauge-field propagator at tree level, given by Eq. (5), and the second term is the gauge field self-energy, given by

$$\Pi^{\mu\nu}(p) = -e^2 \int \frac{d^3k}{(2\pi)^3} \text{Tr}\{\gamma^\mu S_F(k+p)\Gamma^\nu(k,p)S_F(k)\}, \quad (9)$$

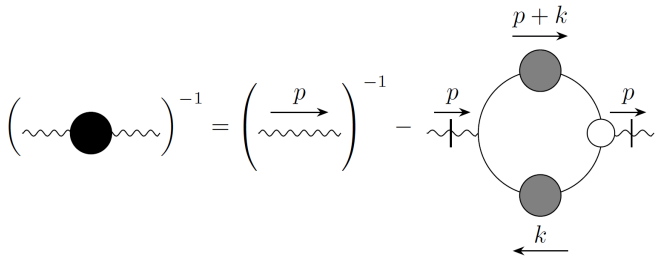


Figure 2. *The Schwinger-Dyson equation for the gauge-field propagator in Eq. (8).* Filled dots represent full propagators and vertex. The black dot corresponds to the full gauge-field propagator, the gray dot to the full fermion propagator, and the white dot to the vertex. The first term on the right-hand side is the bare gauge-field propagator, while the second term represents the gauge-field self-energy  $\Pi^{\mu\nu}(p)$ .

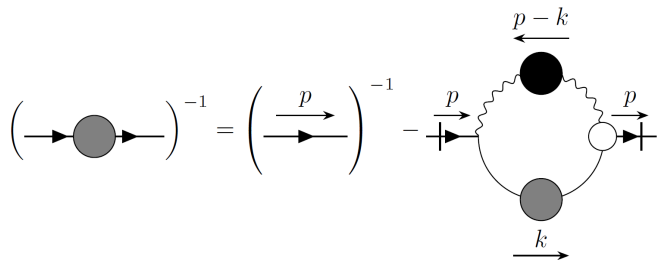


Figure 3. *The Schwinger-Dyson equation for the full electron propagator in Eq. (10).* Filled dots represent full propagators and vertex. The black dot corresponds to the full gauge-field propagator, the gray dot to the full fermion propagator, and the white dot to the vertex. The first term on the right-hand side is the bare fermion propagator and the second term represents the fermion self-energy  $\Xi(p)$ .

where  $\Gamma^\nu(k, p)$  is the full vertex interaction, and  $S_F(p)$  is the full electron propagator. Interestingly, when considering the perturbative approximation, the self-energy for the gauge field  $\Pi_{\mu\nu}(p)$  is given by the vacuum polarization tensor at the lowest-order approximation. In Fig. 2, we show the diagrammatic representation of Eq. (9).

For the fermion propagator, the Schwinger-Dyson equation reads

$$S_F^{-1}(p) = S_{0F}^{-1}(p) - \Xi(p), \quad (10)$$

where

$$\Xi(p) = e^2 \int \frac{d^3k}{(2\pi)^3} \gamma^\mu S_F(k) \Gamma^\nu(k, p) \Delta_{\mu\nu}(p-k) \quad (11)$$

is the electron self-energy. From Eq. (11), we conclude that for calculating the function  $\Xi(p)$ , we would need to know the full gauge-field propagator, which is also dependent on the electron propagator through Eq. (9). We show the diagrammatic representation of this equation in Fig. 3. After taking into account these considerations, it is clear that we need to employ a truncation method for calculating the full electron propagator.

Finally, the Schwinger-Dyson equation for the vertex interaction can be found on pages 10-11 in Ref. [3], however, in this work we will consider the rainbow approximation. This approach consists on the substitution  $\Gamma^\nu(k, p) \rightarrow \gamma^\nu$ , which greatly simplifies the functional form of the vertex interaction by taking only bare term, given by the Dirac matrices [22]. Next, within the called quenched approximation, the fermionic loops are neglected, hence,  $\Pi^{\mu\nu} \rightarrow 0$ , which yields  $\Delta_{\mu\nu} \rightarrow \Delta_{\mu\nu}^0$  by using Eq. (8). This set of approximation is known as the rainbow-quenched approximation and it is a valuable way for calculating dynamical mass generation. This can be improved by considering a gauge field self-energy calculated within the large- $N$  approximation, which is known as the rainbow-unquenched approximation. In principle, this provides better results as long as the condition  $N \gg 1$  is indeed satisfied by the physical system. Several works have confirmed the validity of these approximations after including several corrections, such as a better vertex function, lattice theory, and improved numerical tools [3, 22].

Before we consider these approximations, let us decompose the full electron propagator in terms of two scalar functions, i.e.,

$$S_F^{-1}(p) = -A(p)\not{p} + \Sigma(p), \quad (12)$$

where  $A(p)$  is the renormalized wavefunction of the fermion and  $\Sigma(p)$  is called as mass function. The main motivation for the *ansatz* in Eq. (12) is that it reproduces all of the Lorentz-invariant terms that originally appear into the bare electron propagator. Furthermore, it allows  $\Sigma(p) \neq 0$  even when  $m \rightarrow 0$ , which cannot be realized by a perturbative expansion in PGQED.  $\Sigma(p) \neq 0$  indicates that a dynamical mass is generated and chiral symmetry is broken.

Using Eq. (10), we have

$$S_F^{-1}(p) = -\not{p} + m - \Xi(p). \quad (13)$$

Next, we replace Eq. (12) into Eq. (13) and obtain

$$-A(p)\not{p} + \Sigma(p) = -\not{p} + m - \Xi(p). \quad (14)$$

In order to calculate  $A(p)$  and  $\Sigma(p)$ , we take the trace over the Dirac matrices [23] [3]. After a simple algebra, we find the mass function

$$\Sigma(p) = m - \frac{\text{Tr}\{\Xi(p)\}}{\text{Tr}\{\mathbb{I}\}}, \quad (15)$$

where  $\mathbb{I}$  is the identity matrix. On the other hand, in order to find  $A(p)$ , we multiply Eq. (12) by  $\not{p}$  and take again the trace over the Dirac matrices. Hence, we find

$$A(p) = 1 + \frac{1}{\text{Tr}\{\not{p}^2\}} \text{Tr}\{\not{p} \Xi(p)\}. \quad (16)$$

Note that Eq. (15) and Eq. (16) are two coupled integral equations. The typical approximation used here

is to consider  $A(p) \rightarrow 1$ , which is motivated by two reasons: first, it is a solution for the Ward-Takahashi identity, which relates both the vertex interaction  $\Gamma^\nu(k, p)$  in the rainbow approximation and  $S_F^{-1}(p)$ , hence, it is in agreement with our previous assumptions [22]. Furthermore, it has also a simple interpretation as long as we remember that  $\Xi(p) \sim e^2$  and, therefore, we have

$$A(p) = 1 + \mathcal{O}\left(\frac{e^2}{4\pi}\right). \quad (17)$$

After using Eq. (17) in Eq. (15), it follows that we neglect higher-order contributions such as  $\mathcal{O}(e^4)$  to  $\Xi(p)$  when we take  $A(p) = 1$ . Obviously, this is a perturbative approximation, but it is also in agreement with our previous simplifications. Furthermore, the nonperturbative feature remains well defined due to the arbitrariness of the mass function  $\Sigma(p)$ . Interestingly, from our numerical results, we also conclude that the second term on the rhs of Eq. (16) becomes negligible in the large-external-momentum limit. In this case, it is enough to consider  $A(p) = 1$  (see Appendix B) for calculating a nontrivial solution for  $\Sigma(p)$ . Similar results have been obtained for QED [3, 21, 22] and PQED [2], regarding the function  $A(p)$ .

#### IV. RAINBOW-QUENCHED APPROXIMATION

As we have discussed before, within this approximation, we take  $\Gamma^\mu \rightarrow \gamma^\mu$ ,  $\Delta_{\mu\nu} \rightarrow \Delta_{\mu\nu}^0$ , and  $A(p) \rightarrow 1$  [22]. Therefore, from Eq. (12), the full electron propagator reads

$$S_F(p) = \frac{\not{p} + \Sigma(p)}{p^2 + \Sigma^2(p)}. \quad (18)$$

Furthermore, after some algebra and by using  $m \rightarrow 0$ , Eq. (15) yields

$$\Sigma(p) = 4\pi\alpha \int \frac{d^3k}{(2\pi)^3} \frac{\delta^{\mu\nu}\Sigma(k)}{k^2 + \Sigma^2(k)} \Delta_{\mu\nu}^0(p-k), \quad (19)$$

where we have defined  $e^2 = 4\pi\alpha$ . The constant  $\alpha$  is known as the fine-structure constant and is a dimensionless fundamental constant that characterizes the strength of the electromagnetic interaction between two charged particles [2]. In the context of the Schwinger-Dyson equations, it is relevant for studying dynamical mass generation, because we expect that such effect is realized only in the strongly correlated limit, i.e., for large values of  $\alpha$  [3].

Next, we use Eq. (5) in Eq. (19), within the Landau gauge ( $\xi \rightarrow \infty$ ), hence the mass function reads

$$\Sigma(p) = 4\pi\alpha \int \frac{d^3k}{(2\pi)^3} \frac{\Sigma(k)}{k^2 + \Sigma^2(k)} \times \left[ \frac{1}{\sqrt{(p-k)^2}} - \frac{1}{\sqrt{(p-k)^2 + \mu^2}} \right]. \quad (20)$$

Note that if  $\mu \rightarrow 0$ , that is,  $a \rightarrow \infty$ , then the kernel of the integral vanishes, hence,  $\Sigma(p) \rightarrow 0$  and no dynamical mass is generated.

Thereafter, using spherical coordinates with  $0 \leq \varphi \leq 2\pi$ ,  $0 \leq \eta \leq \pi$ ,  $0 \leq k \leq \Lambda$ ,  $d^3k = k^2 \sin \eta dk d\varphi d\eta$ , and  $(p-k)^2 = p^2 + k^2 - 2kp \cos \eta$ , we find

$$\begin{aligned} \Sigma(p) &= \frac{4\pi\alpha}{(2\pi)^2} \int_0^\Lambda dk \frac{k^2 \Sigma(k)}{k^2 + \Sigma^2(k)} \int_0^\pi d\eta \frac{\sin \eta}{\sqrt{p^2 + k^2 - 2kp \cos \eta}} \\ &- \frac{4\pi\alpha}{(2\pi)^2} \int_0^\Lambda dk \frac{k^2 \Sigma(k)}{k^2 + \Sigma^2(k)} \int_0^\pi d\eta \frac{\sin \eta}{\sqrt{p^2 + k^2 - 2kp \cos \eta + \mu^2}}. \end{aligned} \quad (21)$$

Note that we have included an UV cutoff  $\Lambda$ , which plays an important role for physical applications of our model, as we shall discuss later. After exactly solving the angular integral over  $\eta$ , we obtain

$$\begin{aligned} \Sigma(p) &= \frac{\alpha}{\pi p} \int_0^\Lambda dk \frac{k \Sigma(k)}{k^2 + \Sigma^2(k)} K(p, k) + \\ &- \frac{\alpha}{\pi p} \int_0^\Lambda dk \frac{k \Sigma(k)}{k^2 + \Sigma^2(k)} Q(p, k, \mu), \end{aligned} \quad (22)$$

where we have defined  $K(p, k) = |k+p| - |k-p|$  and  $Q(p, k, \mu) = \sqrt{(k+p)^2 + \mu^2} - \sqrt{(k-p)^2 + \mu^2}$ , which work as kernels to the integral equation for  $\Sigma(p)$ . From these definitions, it follows that

$$K(p, k) = \begin{cases} 2p, & k > p, \\ 2k, & k < p, \end{cases} \quad (23)$$

and

$$Q(p, k, \mu) \approx \begin{cases} \frac{2pk}{(k^2 + \mu^2)^{1/2}}, & k \gg p, \\ \frac{2pk}{(p^2 + \mu^2)^{1/2}}, & k \ll p. \end{cases} \quad (24)$$

In Eqs. (23) and (24), we show the lowest-order contribution for each kernel as an expansion over both the external momentum  $p$  and the loop momentum  $k$ . After using these results in Eq. (22), we find an approximated integral equation for  $\Sigma(p)$ , namely,

$$\begin{aligned} \Sigma(p) &= \frac{2\alpha}{\pi p} \left[ 1 - \frac{p}{(p^2 + \mu^2)^{1/2}} \right] \int_0^p dk \frac{k^2 \Sigma(k)}{k^2 + \Sigma^2(k)} \\ &+ \frac{2\alpha}{\pi} \int_p^\Lambda dk \frac{k \Sigma(k)}{k^2 + \Sigma^2(k)} \left[ 1 - \frac{k}{(k^2 + \mu^2)^{1/2}} \right]. \end{aligned} \quad (25)$$

Obviously, this step is not mandatory for calculating a numerical solution, but it is relevant for an analytical calculation. Here, we should make a few comments about the parameter  $\Lambda$ . Firstly, the term  $\Lambda$  is a UV cutoff that regularizes the theory and allows us to manage the divergences that arise in loop integrals. Indeed, it is an upper limit for the acceptable energies within the physical system, hence, it can be interpreted as a scale beyond which our model is no longer a reasonable approximation [3].

In order to find an analytical solution of Eq. (25), we will convert this integral equation into a differential equation with suitable asymptotic conditions for  $\Sigma(p)$ . Using the Leibniz integral rule in Eq. (25), we can compute the first derivative of  $\Sigma(p)$ , given by

$$\Sigma'(p) = -\frac{2\alpha}{\pi H(p, \mu) p^2} \int_0^p dk \frac{k^2 \Sigma(k)}{k^2 + \Sigma^2(k)}, \quad (26)$$

where, for the sake of simplicity, we define two new functions  $G(p, \mu)$  and  $H(p, \mu)$  that shall be important. These are given by

$$G(p, \mu) = \left[ 1 - \frac{p}{(p^2 + \mu^2)^{1/2}} \right]^{-1} \quad (27)$$

and

$$H(p, \mu) = \left[ 1 - \frac{p^3}{(p^2 + \mu^2)^{3/2}} \right]^{-1}. \quad (28)$$

We can find the IR (infrared) condition by taking the limit  $p \rightarrow 0$  in Eq. (26) and find

$$\lim_{p \rightarrow 0} [H(p, \mu) p^2 \Sigma'(p)] = 0. \quad (29)$$

On the other hand, the UV (ultraviolet) condition could be found by taking the limit  $p \rightarrow \Lambda$  in Eq. (26) and (25), after summing these equations. Therefore, we have

$$\lim_{p \rightarrow \Lambda} [H(p, \mu) p^2 \Sigma'(p) + G(p, \mu) p \Sigma(p)] = 0. \quad (30)$$

Thereafter, we take the second derivative of Eq. (26) and apply the fundamental theorem of calculus on the right-hand side and, after some algebra, we obtain

$$\frac{d}{dp} [H(p, \mu) p^2 \Sigma'(p)] + \frac{2\alpha}{\pi} \frac{p^2 \Sigma(p)}{p^2 + \Sigma^2(p)} = 0, \quad (31)$$

which is a differential equation for the mass function  $\Sigma(p)$ . This must also satisfy both the IR and UV conditions, given by Eqs. (29) and (30), respectively. Even after our set of approximations, Eq. (31) still is a nonlinear differential equation due to the denominator  $p^2 + \Sigma^2(p)$ . This is a typical property of the Schwinger-Dyson equation, where the full propagator is written as a function of itself. Next, we propose a few approximations in order to circumvent this problem.

#### A. Approximations: $p \rightarrow 0$

The simplest approximation would be to consider that the mass function  $\Sigma(p)$  is a constant. From Eq. (25), we conclude that this is a decreasing function of  $p$ , therefore, it is reasonable to assume  $p \rightarrow 0$  to obtain an upper value for the dynamically generated mass. Due to this assumption, we take  $\Sigma(p \rightarrow 0) = M$  in Eq. (25), hence,

$$M = \frac{2\alpha}{\pi} \int_0^\Lambda dk \frac{kM}{k^2 + M^2} - \frac{2\alpha}{\pi} \int_0^\Lambda dk \frac{k^2 M}{k^2 + M^2} \frac{1}{(k^2 + \mu^2)^{1/2}}, \quad (32)$$

which is our gap equation. After solving the integrals over  $k$ , we find

$$\begin{aligned} \frac{\pi}{2\alpha} = & \frac{1}{2} \ln \frac{M^2 + \Lambda^2}{M^2} - \ln \frac{\sqrt{\mu^2 + \Lambda^2} + \Lambda}{\mu} + \\ & + \frac{|M|}{\sqrt{\mu^2 - M^2}} \arctan \frac{\Lambda \sqrt{\mu^2 - M^2}}{|M| \sqrt{\mu^2 + \Lambda^2}}. \end{aligned} \quad (33)$$

It is reasonable to assume that  $\Lambda, \mu \gg M$ , which implies that the third term in the rhs of Eq. (33) is negligible. Therefore,

$$\frac{\pi}{2\alpha} \approx \ln \frac{\Lambda}{|M|} - \ln \frac{\sqrt{\mu^2 + \Lambda^2} + \Lambda}{\mu}, \quad (34)$$

hence,

$$|M| \approx \frac{\Lambda \mu \exp\{-\frac{\pi}{2\alpha}\}}{\Lambda + \sqrt{\Lambda^2 + \mu^2}}. \quad (35)$$

Note that the mass function, given by Eq. (35), vanishes when  $\alpha \rightarrow 0$ , as expected. Furthermore, it is cutoff independent in the limit  $\Lambda \rightarrow \infty$ , yielding a finite value  $M \rightarrow (\mu/2)e^{-\pi/2\alpha}$ . This indicates a better UV behavior of  $M$ , when compared to the known results for PQED. Indeed, after taking  $\mu \rightarrow \infty$  ( $a \rightarrow 0$ ) in Eq. (35), we find  $M \rightarrow \Lambda e^{-\pi/2\alpha}$ , which is a cutoff dependent result and represents the PQED result [2].

#### B. Approximation: $\Sigma^2(p) \gg p^2$

Next, we would like to describe the regime when  $\Sigma(p)$  is not a constant. A simple approximation to the denominator of the second term in the lhs of Eq. (31) is to take  $\Sigma^2(p) \gg p^2$ . This linearizes the differential equation and allow us to calculate an analytical result. Hence, Eq. (31) reduces to

$$\frac{d}{dp} [H(p, \mu) p^2 \Sigma'(p)] \approx 0 \quad (36)$$

whose solution is

$$\begin{aligned} \Sigma(p) = & C \left[ -\frac{1}{p} + \frac{1}{\lambda} + \frac{1}{(p^2 + \mu^2)^{1/2}} - \frac{1}{(\lambda^2 + \mu^2)^{1/2}} \right] + \\ & + \Sigma(\lambda), \end{aligned} \quad (37)$$

where  $C$  and  $\lambda$  are arbitrary constants. Note that if  $p = \lambda$ , then  $\Sigma(p) = \Sigma(\lambda)$ . We obtain the constant  $C$  after using the IR condition, given by Eq. (29), which implies that the only acceptable value is  $C = 0$ . Next, using the UV condition, given by Eq. (30), we conclude that  $\Sigma(p) = \Sigma(\lambda) = 0$ . This means that we cannot describe dynamical mass generation in this approximation and only the trivial phase is a physical solution. The physical reason for such a result is that, for large external momentum, one would need  $\Lambda \ll \Sigma(\Lambda)$ , which is not

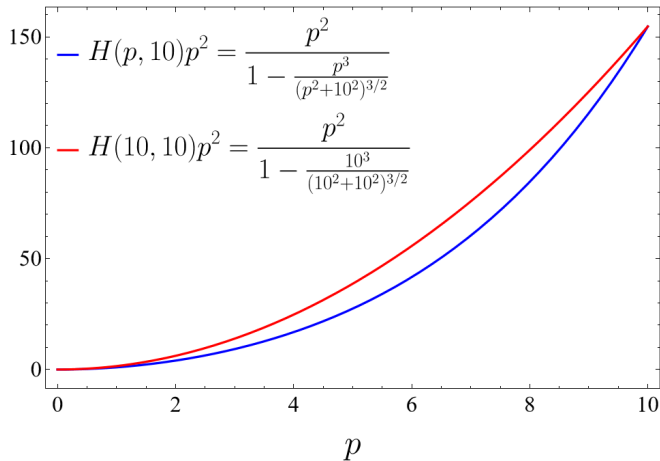


Figure 4. The  $H(p, \mu)p^2 \rightarrow H(\Lambda, \mu)p^2$  approximation within the large-momentum limit in Eq. (38). The blue line shows the exact expression, where we plot  $p^2$  times Eq. (28) for  $\mu = 10$ . The red line corresponds to the large-momentum approximation, plotting  $p^2$  times Eq. (28) for  $\mu = 10$  and  $\Lambda = 10$ . This approximation is valid as long as  $\Lambda > p$  with a finite  $\Lambda$ .

reasonable since it also implies  $\Lambda \ll M$ , where  $M$  is the maximum value of  $\Sigma(p)$ , as we have discussed in the previous approximation. Indeed, we expect that the cutoff is actually much larger than the value of the dynamical mass.

### C. Approximation: $\Sigma^2(p) \ll p^2$

Based on our previous conclusions, the most realistic approximation to the term  $p^2 + \Sigma^2(p)$  would be  $p^2 + \Sigma^2(p) \approx p^2 + M^2$ . This works well for both the small- and large-momentum limits. However, here, we consider only the simplest case where  $\Sigma^2(p) \ll p^2$ , which is enough to describe the mass function, as we shall conclude in this section. We also consider a simplification  $H(p, \mu)p^2 \rightarrow H(\Lambda, \mu)p^2$ , which is a good approximation as long as  $\Lambda > p$ , see Fig. 4. Having in mind these approximations, from Eq. (31), we obtain a Cauchy-Euler differential equation, namely,

$$p^2 \Sigma''(p) + 2p \Sigma'(p) + \frac{2\alpha}{\pi H(\Lambda, \mu)} \Sigma(p) = 0. \quad (38)$$

The solution of this equation reads

$$\Sigma(p) = A_1 p^{\gamma_-} + A_2 p^{\gamma_+}, \quad (39)$$

where  $(A_1, A_2)$  are arbitrary constants,

$$\gamma_{\pm} = -\frac{1}{2} \pm \frac{1}{2} \sqrt{1 - \frac{\alpha}{\alpha_c}} = -\frac{1}{2} \pm i\beta, \quad (40)$$

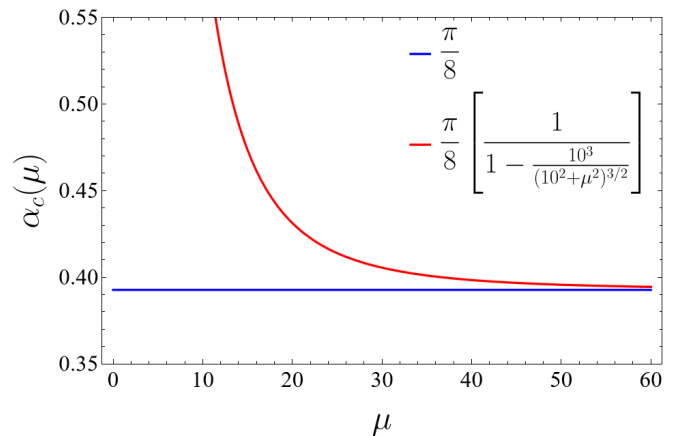


Figure 5. The critical coupling constant of PGQED in Eq. (41). The blue line shows Eq. (41) with  $\mu \rightarrow \infty$ , which corresponds to the critical coupling constant in PQED [2]. The red line shows Eq. (41) for  $\Lambda = 10$ . We observe that as  $\mu$  decreases,  $\alpha_c$  increases which makes dynamical mass generation even harder to be realized because it needs  $\alpha > \alpha_c(\mu)$ .

$$\beta = \frac{1}{2} \sqrt{\frac{\alpha}{\alpha_c} - 1}, \text{ and}$$

$$\alpha_c = \frac{\pi H(\Lambda, \mu)}{8} = \frac{\pi}{8} \left[ \frac{1}{1 - \frac{\Lambda^3}{(\Lambda^2 + \mu^2)^{3/2}}} \right]. \quad (41)$$

The constant  $\alpha_c$ , called the critical coupling constant, defines a threshold above which  $\Sigma(p)$  becomes a decreasing oscillatory function. This regime, when  $\alpha > \alpha_c$ , represents a strongly correlated limit, where chiral symmetry breaking is expected to occur. The Podolsky parameter clearly has an important role for this constant. Indeed, in Fig. 5 we show that for larger values of  $\mu$ , we have  $\alpha_c = \pi/8$ , which is the critical coupling constant for PQED [2]. On the other hand, for small  $\mu$ ,  $\alpha_c$  increases and no dynamical mass generation may occur.

For  $\alpha > \alpha_c$ , the mass function can be written, after some algebra, as

$$\Sigma(p) = \frac{C}{\sqrt{p}} \sin \left[ \beta \left( \ln \frac{p}{\Sigma_0} + \delta \right) \right], \quad (42)$$

where  $B_1 = A_1 + A_2$ ,  $B_2 = A_1 - A_2$ ,  $C = \sqrt{B_1^2 - B_2^2}$ , and  $\delta = \arctan(-iB_1/B_2)$ . Furthermore, a scale factor  $\Sigma_0$  is included due to the logarithmic term. This, on the other hand, can be obtained from the UV condition, given by Eq. (30), after considering the same approximations made to the differential equation. Hence, we have

$$\lim_{p \rightarrow \Lambda} [H(\Lambda, \mu) p^2 \Sigma'(p) + G(\Lambda, \mu) p \Sigma(p)] = 0. \quad (43)$$

After using Eq. (42) in Eq. (43), we obtain

$$\Sigma_0 = \Lambda \exp \left\{ \delta + \frac{2(\Lambda^2 + \mu^2)}{2\Lambda\sqrt{\Lambda^2 + \mu^2} + 3\Lambda^2 + \mu^2} \right\} \times \exp \left\{ \frac{-2n\pi}{\sqrt{\frac{\alpha}{\alpha_c} - 1}} \right\}, \quad (44)$$

where  $n = 0, 1, 2, \dots$  is an integer number. The scale factor in Eq. (44) obeys a Miransky scaling law, whose main feature is that  $\Sigma_0$  is constant for  $\Lambda \rightarrow \infty$  as long as  $\alpha \rightarrow \alpha_c$ , representing an UV fixed point. For  $\alpha < \alpha_c$ , it is straightforward to show that the mass function does not obey the UV condition, hence, the system must remain in the massless phase. This is in agreement with previous results for both QED and PQED. Because  $\alpha_c(\mu)$  is always larger than  $\alpha_c(\infty) = \pi/8$ , it follows that the Podolsky parameter does not favor dynamical mass generation.

## V. RAINBOW-UNQUENCHED APPROXIMATION

As we have discussed before, within this approximation, we take  $\Gamma^\mu \rightarrow \gamma^\mu$ ,  $\Delta_{\mu\nu}$  at lowest order in the large- $N$  expansion, and  $A(p) \rightarrow 1$  [22]. Therefore, the main change is to consider a corrected gauge-field propagator [1, 24].

Firstly, let us show how the vacuum polarization tensor modifies the gauge-field propagator. Within the four-rank representation of Dirac matrices, the vacuum polarization tensor reads

$$\Pi^{\mu\nu}(p, m) = \Pi_1(p, m)P^{\mu\nu}, \quad (45)$$

where the projection operator is given by

$$P_{\mu\nu} = \delta_{\mu\nu} - \frac{p_\mu p_\nu}{p^2}. \quad (46)$$

Using the Schwinger-Dyson equation for the gauge-field propagator in Eq. (8), we obtain

$$\Delta_{\mu\nu} = \Delta_{0\mu\alpha} \{G_\nu^\alpha\}^{-1}, \quad (47)$$

where

$$G_\nu^\alpha = \delta_\nu^\alpha - \Pi^{\alpha\beta} \Delta_{0\beta\nu} = \delta_\nu^\alpha - \Pi_1 P^{\alpha\beta} \Delta_{0\beta\nu}. \quad (48)$$

After some simplifications, we find

$$\Delta_{\mu\nu} = \frac{P_{\mu\nu}}{\left[ \frac{1}{2} \frac{1}{(p^2)^{1/2}} - \frac{1}{2} \frac{1}{(p^2 + \mu^2)^{1/2}} \right]^{-1} - \Pi_1}. \quad (49)$$

For massless fermions  $m \rightarrow 0$ , the function  $\Pi_1(p)$  is [25]

$$\Pi_1(p) = -\frac{g}{8}(p^2)^{1/2}, \quad (50)$$

where  $g \rightarrow e^2 N$  is a coupling constant related to the electric charge  $e$  and to the flavor number of the Dirac

field  $N$ . Note that we could also consider  $g \rightarrow 4\pi\alpha N$  written in terms of the fine-structure constant. The main idea of the large- $N$  expansion is that  $g$  is fixed when  $\alpha \ll 1$  and  $N \gg 1$  [26].

Therefore, the corrected gauge-field propagator is given by

$$\Delta_{\mu\nu} = \frac{P_{\mu\nu}}{\left[ \frac{1}{2} \frac{1}{(p^2)^{1/2}} - \frac{1}{2} \frac{1}{(p^2 + \mu^2)^{1/2}} \right]^{-1} + \frac{g}{8}(p^2)^{1/2}}, \quad (51)$$

where we have used the Landau gauge  $\xi \rightarrow \infty$ . Using these approximations, from Eq. (15), we find that the mass function is given by

$$\Sigma(p) = \frac{g}{N} \int \frac{d^3k}{(2\pi)^3} \frac{\Sigma(k)}{k^2 + \Sigma^2(k)} \delta^{\mu\nu} \Delta_{\mu\nu}(p-k). \quad (52)$$

Using Eq. (51) into Eq. (19), having in mind that  $4\pi\alpha \rightarrow g/N$ , we find

$$\Sigma(p) = \frac{2g}{N} \int \frac{d^3k}{(2\pi)^3} \frac{\Sigma(k)}{k^2 + \Sigma^2(k)} \times \frac{1}{\left[ \frac{1}{2} \frac{1}{\sqrt{(p-k)^2}} - \frac{1}{2} \frac{1}{\sqrt{(p-k)^2 + \mu^2}} \right]^{-1} + \frac{g}{8} \sqrt{(p-k)^2}}. \quad (53)$$

Similarly to the rainbow-quenched approximation, we conclude that when  $\mu \rightarrow 0$  ( $a \rightarrow \infty$ ), the kernel of the integral in Eq. (53) vanishes. Using spherical coordinates for the loop integral, we have

$$\Sigma(p) = \frac{4\pi g}{(2\pi)^3 N} \int_0^\Lambda \int_0^\pi dk d\eta \frac{k^2 \Sigma(k)}{k^2 + \Sigma^2(k)} L(p-k, \eta, \mu, g), \quad (54)$$

where

$$L(q, \eta, \mu, g) = \frac{\sin \eta}{\left[ \frac{1}{2} \frac{1}{\sqrt{q^2}} - \frac{1}{2} \frac{1}{\sqrt{q^2 + \mu^2}} \right]^{-1} + \frac{g}{8} \sqrt{q^2}} \quad (55)$$

is the kernel of the integral and  $q = p - k$ . Next, let us solve the integral equation for  $\Sigma(p)$  using the same momentum expansion applied before.

### A. Approximation: $\Sigma^2(p) \ll p^2$

Firstly, we expand the kernel of the integral equation for both  $k \gg p$  and  $k \ll p$ . Hence, for  $k \gg p$ , we have

$$L(k, \eta, \mu, g) \approx \frac{\sin \eta}{\frac{g\sqrt{k^2}}{8} + \frac{1}{2\sqrt{k^2}} - \frac{1}{2\sqrt{k^2 + \mu^2}}}, \quad (56)$$

while for  $k \ll p$  it reads

$$L(p, \eta, \mu, g) \approx \frac{\sin \eta}{\frac{g\sqrt{p^2}}{8} + \frac{1}{2\sqrt{p^2}} - \frac{1}{2\sqrt{p^2 + \mu^2}}}. \quad (57)$$

This expansion is relevant in order to simplify the angular integral and it is the same level of approximation we have used before in the rainbow-quenched case. Therefore, we have

$$\Sigma(p) = \frac{4\pi g}{(2\pi)^3 N} \int_0^\Lambda \int_0^\pi dk d\eta \frac{k^2 \Sigma(k)}{k^2 + \Sigma^2(k)} \times \left\{ L(k, \eta, \mu, g) \theta(k-p) + L(p, \eta, \mu, g) \theta(p-k) \right\}, \quad (58)$$

where  $\theta(x)$  is the Heaviside step function. After solving the angular integral, we obtain

$$\Sigma(p) = \frac{8\pi g}{(2\pi)^3 N} \int_0^p dk \frac{k^2 \Sigma(k)}{k^2 + \Sigma^2(k)} \left\{ \frac{I(p, \mu, g)}{p} \right\} + \frac{8\pi g}{(2\pi)^3 N} \int_p^\Lambda dk \frac{k^2 \Sigma(k)}{k^2 + \Sigma^2(k)} \left\{ \frac{I(k, \mu, g)}{k} \right\}. \quad (59)$$

where, for the sake of simplicity, we define the function

$$I(p, \mu, g) = \left[ \frac{g}{8} + \frac{1}{\frac{1}{2} - \frac{p}{2\sqrt{p^2 + \mu^2}}} \right]^{-1}. \quad (60)$$

Thereafter, we take the derivative with respect to  $p$  in both sides of Eq. (59), then it follows

$$\frac{J(p, \mu, g)}{I^2(p, \mu, g)} p^2 \Sigma'(p) + \frac{8\pi g}{(2\pi)^3 N} \int_0^p dk \frac{k^2 \Sigma(k)}{k^2 + \Sigma^2(k)} = 0, \quad (61)$$

with

$$J(p, \mu, g) = \left[ \frac{g}{8} - \frac{\frac{p}{2(p^2 + \mu^2)^{3/2}} - \frac{1}{2p^2}}{\left( \frac{1}{2p} - \frac{1}{2\sqrt{p^2 + \mu^2}} \right)^2} \right]^{-1}, \quad (62)$$

an auxiliary function. The next derivative in respect to  $p$  yields

$$\frac{d}{dp} \left[ \frac{J(p, \mu, g)}{I^2(p, \mu, g)} p^2 \Sigma'(p) \right] + \frac{8\pi g}{(2\pi)^3 N} \frac{p^2 \Sigma(p)}{p^2 + \Sigma^2(p)} = 0. \quad (63)$$

Similarly to the rainbow-quenched case, we consider  $\Sigma^2(p) \ll p^2$  and

$$\frac{J(p, \mu, g)}{I^2(p, \mu, g)} p^2 \rightarrow \frac{J(\Lambda, \mu, g)}{I^2(\Lambda, \mu, g)} p^2 \quad (64)$$

in order to obtain a Cauchy-Euler differential equation, given by

$$p^2 \Sigma''(p) + 2p \Sigma'(p) + \frac{I^2(\Lambda, \mu, g)}{J(\Lambda, \mu, g)} \frac{g}{\pi^2 N} \Sigma(p) = 0. \quad (65)$$

The solution of Eq. (65) reads

$$\Sigma(p) = E_1 p^{\gamma_-} + E_2 p^{\gamma_+}, \quad (66)$$

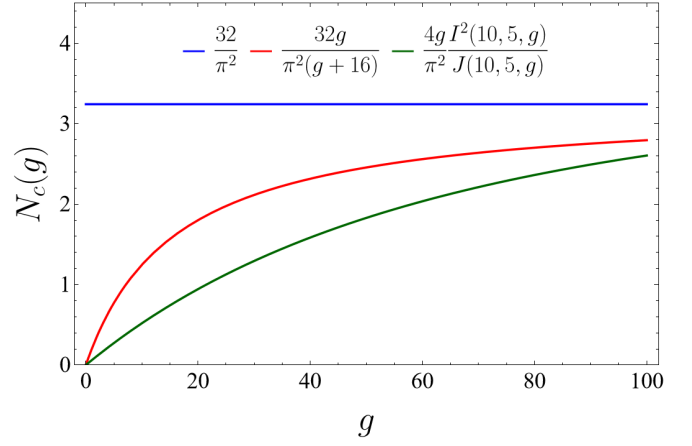


Figure 6. The critical coupling constant of PGQED in Eq. (68). The blue line shows Eq. (68) with  $\mu \rightarrow \infty$  and  $g \rightarrow \infty$ , which corresponds to the critical coupling constant in QED3 [1]. The red line shows Eq. (68) with  $\mu \rightarrow \infty$ , which corresponds to the critical coupling constant in PQED [2]. The green line shows Eq. (68) for  $\Lambda = 10$  and  $\mu = 5$ . We observe that the function has an upper limit, and  $N_c$  increases, as  $g$  increases.

where  $(E_1, E_2)$  are arbitrary constants,

$$\gamma_{\pm} = -\frac{1}{2} \pm \frac{1}{2} \sqrt{1 - \frac{N_c}{N}} = -\frac{1}{2} \pm i\beta, \quad (67)$$

with  $\beta = \frac{1}{2} \sqrt{\frac{N_c}{N} - 1}$ , and

$$N_c = \frac{4g}{\pi^2} \frac{I^2(\Lambda, \mu, g)}{J(\Lambda, \mu, g)} = \frac{4g}{\pi^2} \frac{\left[ g/8 + \frac{y_{1/2}^2(\Lambda, \mu)}{y_{3/2}(\Lambda, \mu)} \right]}{\left[ g/8 + y_{1/2}(\Lambda, \mu) \right]^2}, \quad (68)$$

which is the critical number for fermions, below which we expect to obtain a dynamical mass generation, and

$$y_x(\Lambda, \mu) = \left[ \frac{1}{2} - \frac{1}{2} \left( \frac{\Lambda^2}{\Lambda^2 + \mu^2} \right)^x \right]^{-1}, \quad (69)$$

is an auxiliary function.

Note that for large  $\mu \gg \Lambda$  ( $a\Lambda \ll 1$ ), we have  $N_c \rightarrow \frac{32g}{\pi^2(g+16)}$ , which is the same result of PQED in the rainbow-unquenched approximation [2]. We can also see this behavior in Figure 6. Interestingly, when  $g \gg 1$ , we have  $N_c \rightarrow 32/\pi^2$ , which is the critical number for QED in (2+1)D [1]. From Eq. (68), we also may conclude that  $N_c \rightarrow 0$  when  $\mu \ll \Lambda$  ( $a\Lambda \gg 1$ ), hence, no dynamical mass generation occurs. Indeed, for  $N > N_c$  there is no chiral symmetry breaking, which is a consequence of the boundary conditions, given by

$$\lim_{p \rightarrow \Lambda} [J(p, \mu, g) p \Sigma'(p) + I(p, \mu, g) \Sigma(p)] = 0 \quad (70)$$

in the UV limit, and

$$\lim_{p \rightarrow 0} \left[ \frac{J(p, \mu, g)}{I^2(p, \mu, g)} p^2 \Sigma'(p) \right] = 0 \quad (71)$$

in the IR regime. Following the same steps as before, we

also obtain a scale parameter  $\bar{\Sigma}_0$ , given by

$$\bar{\Sigma}_0 = \Lambda \exp \left\{ \bar{\delta} + \frac{2 \left( -g\Lambda\sqrt{\Lambda^2 + \mu^2} + (g+16)\Lambda^2 + (g+16)\mu^2 \right)}{-(g-32)\Lambda\sqrt{\Lambda^2 + \mu^2} + (g+48)\Lambda^2 + (g+16)\mu^2} \right\} \exp \left\{ \frac{-2n\pi}{\sqrt{\frac{N_c}{N} - 1}} \right\}, \quad (72)$$

where  $\bar{\delta}$  is a function of  $(E_1, E_2)$  and  $n = 0, 1, 2, \dots$  is an integer number. The scale in Eq. (72) is a real finite number only if  $N < N_c$  and has been calculated in the limit  $N \approx N_c$  ( $\beta \approx 0$ ).

## VI. SUMMARY AND DISCUSSIONS

We have shown that chiral symmetry breaking occurs in PGQED in the strong-coupling limit, which is obtained when the coupling constant is larger than a critical value, i.e.,  $\alpha > \alpha_c(\mu) = H(\Lambda, \mu)\pi/8$ , where  $H(\mu, \Lambda) \geq 1$  is a known function within the rainbow-quenched approximation. Similar results have been derived when quantum corrections are included in the gauge-field propagator, using the large- $N$  expansion. In this case, with  $g \rightarrow \infty$  (strong interactions), we obtain a critical point  $N_c = 32/\pi^2$ , which is exactly the same critical point obtained earlier for QED in (2+1)D [1, 3, 22]. This has also been observed for PQED and it seems to indicate that, within this asymptotically-large-coupling limit, the electron-electron interaction is actually dominated by the vacuum polarization tensor for a massless electron. Indeed, the corrected gauge-field propagator for a gauge theory with a U(1) interaction would be like  $\propto 1/(G(p^2) + gp)$  in the large- $N$  expansion, where  $G(p^2)$  is the momentum function of the bare gauge-field propagator of these kind of models in (2+1)D, for example: QED ( $G \propto p^2$ ); PQED ( $G \propto \sqrt{p^2}$ ), and; PGQED (See Eq. (49)). On the other hand, the term  $gp$  is the contribution from the vacuum polarization tensor for massless fermion, which does not depend on the gauge-field propagator at one-loop approximation. Hence, whenever  $gp \gg G(p^2)$  ( $g \rightarrow \infty$ ), all of these gauge-field propagators would behave similarly and are expected to generate the same critical number (or closely the same value). This is just a simplistic point of view and a deeper reason could be obtained in future works.

Recently, the author in Ref. [17] has performed a dimensional reduction in the Lee-Wick electrodynamics from (3+1)D to (2+1)D. This calculation yields the same reduced gauge-field propagator we have obtained here, given by Eq. (5) in momentum space, although the starting action in (3+1)D is slightly different from ours. However, they are dual because the electrons interact through the same static potential  $V(r) \propto (1 - e^{-\mu r})/r$ . In Ref. [17], it is also shown that this kind of model respects the microcausality at tree level, which is a desirable feature

for a well-defined field theory. Here, our main results depend on the strength of quantum correction and are likely to be the same in the context of the reduced Lee-Wick electrodynamics, given the similarity of its gauge-field propagator in comparison to the one in PGQED. Obviously, our main results obtained here only hold for an initially massless Dirac field.

The emerging of gauge theories in low dimensions has also been largely discussed in the context of quantum simulations with ultracold atoms. Interestingly, a proposal for realization of QED in two spatial dimensions, using a mixture of ultracold atoms trapped in an optical lattice, has been discussed in Ref. [27]. Possible experimental setups and lattice gauge theories have been discussed for quantum computation in Refs. [28, 29]. Our action in PGQED is a useful example of an emerging gauge theory as it is defined by a pseudo-differential operator. This, on the other hand, yields a richer kind of static interaction among electrons and further generalizations are straightforward. Furthermore, we have two main parameters  $\Lambda$  and  $\mu$ , which can be related to the lattice and to the mass of the boson field, respectively. In the realm of ultracold atoms, the strength of interactions (in our case the fine-structure constant  $\alpha$ ) is expected to be tunable, which opens the possibility of observing non-perturbative effects. Nevertheless, the precise values of these constants depend on details of the system and continuum versions ( $a_L \rightarrow 0$ ) of these lattice models could be important for a better comparison. For the best of our knowledge, such models are currently unknown, but we believe that PQED-like gauge theories could be important candidates.

One relevant application of mass generation in PGQED would be the opening of an electronic band gap in graphene in the ultrarelativistic limit, where electrons move at the speed of light and Lorentz symmetry is respected. This limit is more realistic for samples with a very small density of charge carriers, as has been experimentally shown in Ref. [18]. For graphene, the massless Dirac action is promptly obtained as a low-energy approximation of charge carriers. This is in agreement with our model for the matter field, which interact with the static potential in Eq. (4). Next, let us discuss how to estimate the main system-dependent constants ( $\Lambda, \mu, \alpha$ ) for this material. For PGQED, the Podolsky parameter  $\mu$  can be understood as a phenomenological parameter that decreases the strength of the Coulomb potential, which is a reasonable effect due to the many-body physics of

the problem. Indeed, our parameter  $\mu$  can be used to explain the upper limit of the possible gap in graphene  $2|M| \leq 0.1$  meV, reported in the experimental work in Ref. [18]. In this case,  $\Lambda \approx 1$  eV is obtained from the inverse of the lattice parameter  $a_L \approx 10^{-10}$  m. The fine-structure constant for suspended monolayer graphene is known to be close to  $\alpha \approx 2.2$  [5]. Using these values in Eq. (35) with  $2|M| = 0.1$  meV we obtain the value of the Podolsky parameter, namely,  $\mu = 0.2$  meV. We may conclude that the parameter  $\mu$  in our model is a useful tool because the true many-body interaction among electrons in graphene (and other two-dimensional materials) is not known, but it is expected to have a screened Coulomb potential due to the electromagnetic interaction. Indeed, large values of the dielectric constant have been reported in Ref. [18] for graphene placed above another material.

Finally, we conclude that our work also clarifies how one may realize a dimensional reduction of a model with higher-order derivative terms, where we have shown that the same method used for QED in (3+1)D (resulting in PQED) also holds for the GQED (resulting in PGQED). Having applications for graphene in mind, one could also include a Fermi velocity  $v_F \neq c$  such that the Lorentz symmetry is broken. Inclusion of external magnetic fields should also play a relevant role to describe the quantum Hall effect in two-dimensional materials [30, 31]. We shall discuss this elsewhere.

## ACKNOWLEDGEMENT

C. A. P. C. J. is partially supported by Coordenação de Aperfeiçoamento de Pessoal de Nível Superior Brasil (CAPES), finance code 001. L. O. N. and V. S. A. are partially supported by Conselho Nacional de Desenvolvimento Científico e Tecnológico-Brazil (CNPq-Brazil), process: 408735/2023-6 CNPq/MCTI.

## Appendix A: THE DIMENSIONAL REDUCTION OF GQED

In this appendix, we derive the dimensional reduction of GQED theory from (3+1)D to (2+1)D. Firstly, let us define the action of GQED in (3+1)D in the Euclidean spacetime, namely,

$$\mathcal{L}_P = \frac{1}{4} F_{\mu\nu} F^{\mu\nu} - \frac{a^2}{2} \partial_\nu F^{\mu\nu} \partial^\sigma F_{\mu\sigma} + \frac{\lambda}{2} (\partial_\mu A^\mu)^2, \quad (\text{A.1})$$

where  $a$  is the Podolsky parameter,  $A_\mu$  is the gauge field, and  $F_{\mu\nu} = \partial_\mu A_\nu - \partial_\nu A_\mu$  is its strength tensor. Furthermore,  $\lambda$  is the gauge fixing parameter. Next, after neglecting total derivative terms, we find

$$\begin{aligned} \frac{1}{4} F_{\mu\nu} F^{\mu\nu} + \frac{\lambda}{2} (\partial_\mu A^\mu)^2 &= -\frac{1}{2} \delta_{\mu\nu} A^\mu \square A^\nu + \\ &+ \frac{1}{2} (1 - \lambda) A^\mu \partial_\mu \partial_\nu A^\nu. \end{aligned} \quad (\text{A.2})$$

On the other hand, for the Podolsky term, we have

$$\partial_\nu F^{\mu\nu} \partial^\sigma F_{\mu\sigma} = A^\mu (\partial_\mu \partial_\nu \square) A^\nu - \delta_{\mu\nu} A^\mu (\square \square) A^\nu. \quad (\text{A.3})$$

Hence, it follows that

$$\mathcal{L}_P = \frac{1}{2} A^\mu [(-\square)(1 - a^2 \square) \delta_{\mu\nu} + (1 - \lambda - a^2 \square) \partial_\mu \partial_\nu] A^\nu. \quad (\text{A.4})$$

Next, we write the GQED action as

$$\mathcal{L}_P = \frac{1}{2} A^\mu \Delta_{0,\mu\nu}^{-1} A^\nu, \quad (\text{A.5})$$

where  $\Delta_{0,\mu\nu}^{-1}$  is the inverse of the gauge-field propagator, given by

$$\Delta_{0,\mu\nu}^{-1} = (-\square)(1 - a^2 \square) \delta_{\mu\nu} + (1 - \lambda - a^2 \square) \partial_\mu \partial_\nu. \quad (\text{A.6})$$

After we calculate the Fourier transform of this propagator, using  $\square \rightarrow -p^2$  and  $\partial_\mu \rightarrow -ip_\mu$ , we find

$$\Delta_{0,\mu\nu}^{-1}(p) = p^2(1 + a^2 p^2) \delta_{\mu\nu} - (1 - \lambda + a^2 p^2) p_\mu p_\nu. \quad (\text{A.7})$$

Therefore, the bare gauge-field propagator reads

$$\Delta_{\mu\nu}^0(p) = \frac{1}{p^2(1 + a^2 p^2)} \left[ \delta_{\mu\nu} - \frac{p_\mu p_\nu}{p^2} \right] + \frac{1}{\lambda} \frac{p_\mu p_\nu}{p^4}. \quad (\text{A.8})$$

In order to perform the dimensional reduction, we start from the generating functional of the Green functions of the electron propagator in the theory. Therefore, we define

$$Z = Z_0 \int DA_\mu D\psi D\bar{\psi} e^{-\int d^4x [\mathcal{L}_P + \mathcal{L}_F - e j_\mu A^\mu - \bar{\psi} \eta - \bar{\eta} \psi]}, \quad (\text{A.9})$$

where  $\mathcal{L}_F$  is the fermionic Lagrangian,  $Z_0$  is a normalization constant,  $j_\mu = \bar{\psi} \gamma_\mu \psi$  is the matter current,  $\eta$  and  $\bar{\eta}$  are sources for the fermionic field. Using our previous results, it is straightforward that

$$\begin{aligned} Z &= Z_0 \int D\psi D\bar{\psi} e^{-\int d^4x [\mathcal{L}_F - \bar{\psi} \eta - \bar{\eta} \psi]} \times \\ &\times \int DA_\mu e^{-\int d^4x [\frac{1}{2} A^\mu \Delta_{0,\mu\nu}^{-1} A^\nu - e j_\mu A^\mu]}. \end{aligned} \quad (\text{A.10})$$

The functional integral over  $A_\mu$  can be solved by using the identity

$$\int D\varphi e^{-\frac{1}{2} \int d^4x [\varphi \Delta \varphi] + \int d^4x J \varphi} = \det \Delta^{-1/2} e^{\frac{1}{2} \int d^4x [J \Delta^{-1} J]}, \quad (\text{A.11})$$

where  $\varphi$  is a real bosonic field,  $\Delta$  is an arbitrary matrix, and  $J$  is a source term for the field  $\varphi$ . Let us define  $I$  as the relevant integral in Eq. (A.10), hence,

$$\begin{aligned} I &= \int DA_\mu e^{-\int d^4x [\frac{1}{2} A^\mu \Delta_{0,\mu\nu}^{-1} A^\nu - e j_\mu A^\mu]} \\ &= \int DA_\mu e^{-\frac{1}{2} \int d^4x [A^\mu \Delta_{0,\mu\nu}^{-1} A^\nu] + \int d^4x j_\mu (e A^\mu)} \\ &= \frac{1}{e} \int D(e A_\mu) e^{-\frac{1}{2} \int d^4x [(e A^\mu) \frac{\Delta_{0,\mu\nu}^{-1}}{e^2} (e A^\nu)] + \int d^4x j_\mu (e A^\mu)} \\ &= \frac{1}{e} \det \{ \Delta_{0,\mu\nu}^{-1} / e^2 \}^{-4/2} e^{\int d^4x d^4y [\frac{e^2}{2} j^\mu \Delta_{0,\mu\nu} j^\nu]}. \end{aligned} \quad (\text{A.12})$$

After a simple scaling  $Z_0 \rightarrow Z'_0$  in the normalization constant, the generating functional becomes

$$Z = Z'_0 \int D\bar{\psi} D\psi e^{-\int d^4x d^4y \left[ -\frac{e^2}{2} j^\mu \Delta_{0,\mu\nu} j^\nu + \dots \right]}, \quad (\text{A.13})$$

where the dots in the rhs of Eq. (A.13) mean terms that depend only on the matter field and, therefore, does not change our main result.

Next, we confine the matter current to a plane  $x_1 - x_2$ , which is performed by considering

$$j_\mu = \begin{cases} j_\mu^{3D}(x_0, x_1, x_2) \delta(x_3), & \mu = 0, 1, 2 \\ 0, & \mu = 3. \end{cases} \quad (\text{A.14})$$

Using Eq. (A.14) in Eq. (A.13), we realize that the effective gauge-field propagator is given by

$$\begin{aligned} \Delta_{\mu\nu}^0(x, y) \Big|_{x_3=y_3=0} &= \int \frac{d^4k}{(2\pi)^4} \frac{\delta_{\mu\nu} e^{ik(x-y)}}{k^2(1+a^2k^2)} \Big|_{x_3=y_3=0} \\ &= \frac{1}{2} \frac{\delta_{\mu\nu}}{(-\square)^{1/2}} - \frac{1}{2} \frac{\delta_{\mu\nu}}{(-\square + \mu^2)^{1/2}}, \end{aligned} \quad (\text{A.15})$$

where we have used the identity

$$\frac{1}{k^2(1+a^2k^2)} = \frac{1}{k^2} - \frac{a^2}{1+a^2k^2} = \frac{1}{k^2} - \frac{1}{k^2 + \mu^2}, \quad (\text{A.16})$$

and  $\mu = 1/a$  where  $\square$  now denotes the d'Alembertian operator in (2+1)D. It turns out that the same result in Eq. (A.13) can also be obtained by the following action in (2+1)D, namely,

$$\mathcal{L}_{\text{PGQED}} = \frac{1}{4} \tilde{F}_{\mu\nu} K_E[\square] \tilde{F}^{\mu\nu} + \frac{\xi}{2} \partial_\mu \tilde{A}^\mu K[\square] \partial_\nu \tilde{A}^\nu + \mathcal{L}_F + \mathcal{L}_I, \quad (\text{A.17})$$

where  $\xi$  is a gauge-fixing parameter,  $\mathcal{L}_I$  is the standard interaction of QED, and

$$K_E[\square] = \frac{2(-\square + \mu^2)}{(-\square + \mu^2)(-\square)^{1/2} - (-\square)(-\square + \mu^2)^{1/2}} \quad (\text{A.18})$$

is a pseudo-differential operator. This concludes our derivation of PGQED, given by Eq. (A.17).

## Appendix B: NUMERICAL SOLUTION OF NONLINEAR INTEGRAL EQUATION

In this appendix, we discuss the numerical solutions of the integral equation for  $\Sigma(p)$  in both Eq. (22) and Eq. (54), obtained in the rainbow-quenched and rainbow-unquenched approximations, respectively. These solutions are obtained after converting the integral over  $k$  into a sum over a discretized variable  $k_n \in [p_{\min}, \Lambda]$ , where  $p_{\min} = 10^{-3}$  (in units of  $\Lambda$ ) and  $\Lambda = 10$ . Thereafter, we use the repeated trapezoidal quadrature rule and solve a set of algebraic equations for  $\Sigma(p)$  for each value of  $p$ , which is discretized such as  $k_n$ . We also choose  $M = 300$  as the number of intervals for  $k_n$ , hence,  $n = 1, \dots, M$  with a separation of approximately  $h = (10 - 10^{-3})/(300 - 1) \approx 0.033$  between  $k_n$  and  $k_{n+1}$ . The same method has been applied in previous works for PQED in several different cases Refs. [2, 32].

In Fig. 7, we show the numerical results for PGQED within the quenched-rainbow approximation. Furthermore, we also plot the analytical solution in Eq. (39), for  $\alpha > \alpha_c$ , in order to compare the analytical to the numerical results. Our numerical results indicate that the mass function is much less than  $\Lambda$  for  $\alpha < \alpha_c$  and it increases for  $\alpha > \alpha_c$  until it becomes a small fraction of the UV cutoff. The calculated  $\alpha_c$  in Eq. (41) yields a reasonable estimate for the critical coupling constant, in particular, it describes the role of the Podolsky parameter  $a = 1/\mu$ . However, as it has been discussed in Refs. [3, 22], other approximations may provide other critical coupling constants, for example, by modifying the approximation for the vertex interaction and for  $A(p)$ . The physical interpretation of  $\alpha_c$ , however, it is the same as we discuss here. The analytical mass function  $\Sigma(p)$  has a very close behavior in comparison to the numerical results, which is in agreement with previous results for QED3 in Ref. [33]. In Fig. (8), we confirm these main results, but for the rainbow-unquenched approximation.

Next, we discuss the numerical solution for wavefunction renormalization  $A(p)$  within the quenched-rainbow approximation in the symmetric phase  $\Sigma(p) = 0$ . From Eq. (16) and Eq. (11), after taking the trace over the  $\gamma_\mu$  matrices, we find

$$\begin{aligned} A(p) &= 1 + \frac{\alpha}{\pi p^2} \int_0^{+\infty} \frac{dk}{A(k)} \int_0^\pi d\theta \sin \theta \left[ \frac{1}{\sqrt{p^2 + k^2 - 2pk \cos \theta}} - \frac{1}{\sqrt{p^2 + k^2 - 2pk \cos \theta + \mu^2}} \right] \times \\ &\times \frac{[p^3 k \cos \theta - k^2 p^2 \cos^2 \theta - p^2 k^2 + k^3 p \cos \theta]}{p^2 + k^2 - 2pk \cos \theta}. \end{aligned} \quad (\text{B.1})$$

From Fig. 9, we conclude that the wavefunction renor-

malization is approximately equal to one, hence,  $A(p) \approx$

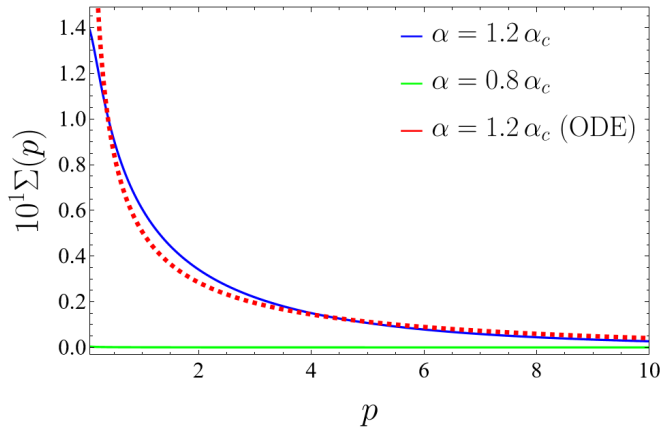


Figure 7. Numerical and analytical results for PGQED in the quenched-rainbow approximation. The blue and green lines are the numerical solutions of Eq. (22) as functions of the external momentum  $p$  with  $\alpha = 1.2\alpha_c$  and  $\alpha = 0.8\alpha_c$ , respectively. We consider  $\mu = 8$  and  $\Lambda = 10$ , which gives  $\alpha_c = 0.75$  from Eq. (41). The red dashed line shows the analytical solution from Eq. (39), with  $A_1 = 0.25 - 0.32i$  and  $A_2 = 0.25 + 0.32i$ , which agrees well with the numerical solutions for  $\alpha = 1.2\alpha_c$  when  $p$  is large.

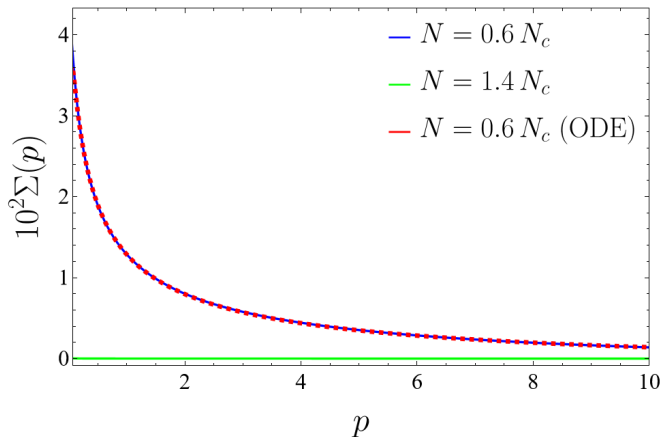


Figure 8. Numerical and analytical results for PGQED in the unquenched-rainbow approximation. The blue and green lines are the numerical solutions of Eq. (53) for  $N = 0.6N_c$  and  $N = 1.4N_c$ , respectively. We consider  $\mu = 8$ ,  $g = 70$  and  $\Lambda = 10$ , which implies from Eq. (68) that  $N_c = 2.71$ . The red dashed line corresponds to the analytical solution from Eq. (66), with  $E_1 = 0.64 - 0.19i$  and  $E_2 = 0.64 + 0.19i$ , which is consistent with the numerical solutions for  $N = 0.6N_c$ .

1 is indeed a good approximation within the large-external-momentum case.

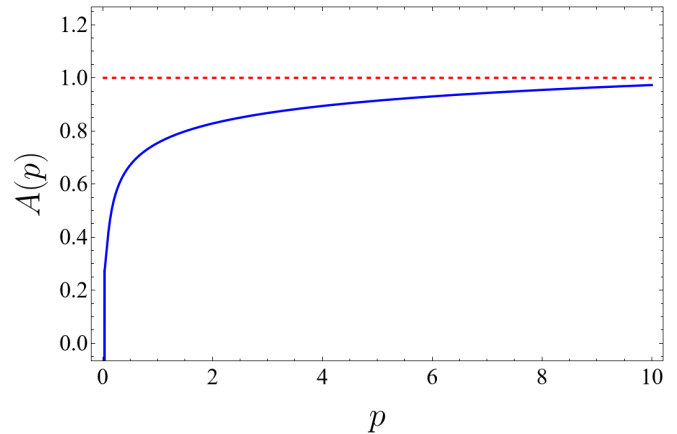


Figure 9. Numerical results for the wavefunction renormalization  $A(p)$ . The blue line is the numerical solution of Eq. (B.1), within both the quenched-rainbow approximation and the symmetric phase  $\Sigma(p) = 0$ . We consider  $\mu = 1000$ ,  $\alpha_c = 0.39$  and  $\alpha = 1.2\alpha_c$ . Note that  $A(p) \rightarrow 1$  when  $p \rightarrow \Lambda$ .

- [1] T. Appelquist, M. J. Bowick, E. Cohler, and L. C. R. Wijewardhana, Chiral-symmetry breaking in 2+1 dimensions, *Physical Review Letters* **55**, 1715 (1985).
- [2] V. S. Alves, W. S. Elias, L. O. Nascimento, V. Juričić, and F. Peña, Chiral symmetry breaking in the pseudo-quantum electrodynamics, *Physical Review D* **87**, 125002 (2013).
- [3] C. D. Roberts and A. G. Williams, Dyson-schwinger equations and their application to hadronic physics, *Progress in Particle and Nuclear Physics* **33**, 477 (1994).
- [4] K. S. Novoselov, A. K. Geim, S. V. Morozov, D. Jiang, M. I. Katsnelson, I. V. Grigorieva, S. V. Dubonos, and A. A. Firsov, Two-dimensional gas of massless dirac fermions in graphene, *Nature* **438**, 197 (2005).
- [5] A. H. C. Neto, F. Guinea, N. M. R. Peres, K. S. Novoselov, and A. K. Geim, The electronic properties of graphene, *Reviews of Modern Physics* **81**, 109 (2009).
- [6] V. P. Gusynin, S. G. Sharapov, and J. P. Carbotte, Ac conductivity of graphene: From tight-binding model to 2 + 1-dimensional quantum electrodynamics, *International Journal of Modern Physics B* **21**, 4611 (2007).
- [7] E. Marino, Quantum electrodynamics of particles on a plane and the chern-simons theory, *Nuclear Physics B* **408**, 551 (1993).
- [8] J. D. L. Silva, A. N. Braga, W. P. Pires, V. S. Alves, D. T. Alves, and E. Marino, Inhibition of the fermi velocity renormalization in a graphene sheet by the presence of a conducting plate, *Nuclear Physics B* **920**, 221 (2017).
- [9] J. D. L. Silva, A. N. Braga, W. P. Pires, D. T. Alves, and V. S. Alves, Renormalization of fermi velocity and band gap in a two-dimensional system near a conducting plate at finite temperature, *Condensed Matter* **9**, 50 (2024).
- [10] L. Fernández, V. S. Alves, L. O. Nascimento, F. Peña, M. Gomes, and E. C. Marino, Renormalization of the band gap in 2d materials through the competition between electromagnetic and four-fermion interactions in large n expansion, *Physical Review D* **102**, 016020 (2020).
- [11] L. Fernández, V. S. Alves, M. Gomes, L. O. Nascimento, and F. Peña, Influence of the four-fermion interactions in a  $(2 + 1)$  d massive electron system, *Physical Review D* **103**, 105016 (2021).
- [12] N. Bezerra, V. S. Alves, L. O. Nascimento, and L. Fernández, Effects of the two-dimensional coulomb interaction in both fermi velocity and energy gap for dirac-like electrons at finite temperature, *Physical Review D* **108**, 056012 (2023).
- [13] N. Menezes, V. S. Alves, E. C. Marino, L. Nascimento, L. O. Nascimento, and C. M. Smith, Spin g-factor due to electronic interactions in graphene, *Physical Review B* **95**, 245138 (2017).
- [14] G. C. Magalhães, V. S. Alves, L. O. Nascimento, and E. C. Marino, Bosonization, mass generation, and the pseudo-chern-simons action, *Physical Review D* **103**, 116022 (2021).
- [15] B. Podolsky and C. Kikuchi, A generalized electrodynamics part ii—quantum, *Physical Review* **65**, 228 (1944).
- [16] M. Fonseca and A. Paredes, Is it possible to accommodate massive photons in the framework of a gauge-invariant electrodynamics?, *Brazilian Journal of Physics* **40**, 319 (2010).
- [17] M. Neves, Classical features, anderson-higgs mechanism, and unitarity in lee-wick pseudo-electrodynamics, *Physical Review D* **111**, 016009 (2025).
- [18] D. C. Elias, R. V. Gorbachev, A. S. Mayorov, S. V. Morozov, A. A. Zhukov, P. Blake, L. A. Ponomarenko, I. V. Grigorieva, K. S. Novoselov, F. Guinea, and A. K. Geim, Dirac cones reshaped by interaction effects in suspended graphene, *Nature Physics* **7**, 701 (2011).
- [19] P. H. Ortega, *A Pseudo Eletrodinâmica de Podolsky*, Ph.D. thesis, Federal University of Rio de Janeiro (2018).
- [20] E. C. Marino, *Quantum Field Theory Approach to Condensed Matter Physics*, 1st ed. (Cambridge University Press, 2017) p. 532.
- [21] P. Maris, Confinement and complex singularities in three-dimensional qed, *Physical Review D* **52**, 6087 (1995).
- [22] P. Maris, Influence of the full vertex and vacuum polarization on the fermion propagator in  $(2+1)$ -dimensional qed, *Physical Review D* **54**, 4049 (1996).
- [23] In  $(2+1)$ D Euclidean space and in the  $4 \times 4$  representation:  $\text{Tr}(\gamma^\mu, \gamma^\nu) = -4\delta^{\mu\nu}$ ,  $\text{Tr}(\gamma^\mu, \gamma^\nu, \gamma^\alpha) = 0$ , and  $\text{Tr}(\gamma^\mu, \gamma^\nu, \gamma^\alpha, \gamma^\beta) = 4(\delta^{\mu\nu}\delta^{\alpha\beta} - \delta^{\mu\alpha}\delta^{\nu\beta} + \delta^{\mu\beta}\delta^{\nu\alpha})$ .
- [24] D. Montenegro, Vacuum polarization of generalized quantum electrodynamics in the heisenberg picture, *International Journal of Modern Physics A* **35**, 2050012 (2020).
- [25] K.-I. Kondo and P. Maris, Spontaneous chiral-symmetry breaking in three-dimensional qed with a chern-simons term, *Physical Review D* **52**, 1212 (1995).
- [26] S. Coleman, *Aspects of Symmetry*, 1st ed. (Cambridge University Press, 1985) p. 420.
- [27] R. Ott, T. V. Zache, F. Jendrzejewski, and J. Berges, Scalable cold-atom quantum simulator for two-dimensional qed, *Physical Review Letters* **127**, 130504 (2021).
- [28] J. C. Halimeh, M. Aidelsburger, F. Grusdt, P. Hauke, and B. Yang, Cold-atom quantum simulators of gauge theories, *Nature Physics* **21**, 25 (2025).
- [29] M. Meth, J. Zhang, J. F. Haase, C. Edmunds, L. Postler, A. J. Jena, A. Steiner, L. Dellantonio, R. Blatt, P. Zoller, T. Monz, P. Schindler, C. Muschik, and M. Ringbauer, Simulating two-dimensional lattice gauge theories on a qudit quantum computer, *Nature Physics* **21**, 570 (2025).
- [30] E. Rojas, A. Ayala, A. Bashir, and A. Raya, Dynamical mass generation in qed with magnetic fields: Arbitrary field strength and coupling constant, *Physical Review D* **77**, 093004 (2008).
- [31] N. Menezes, V. S. Alves, and C. M. Smith, The influence of a weak magnetic field in the renormalization-group functions of  $(2 + 1)$ -dimensional dirac systems, *The European Physical Journal B* **89**, 271 (2016).
- [32] L. O. Nascimento, V. S. Alves, F. Peña, C. M. Smith, and E. C. Marino, Chiral-symmetry breaking in pseudo-quantum electrodynamics at finite temperature, *Physical Review D* **92**, 025018 (2015).
- [33] P. Maris, Dynamical mass generation in qed3 with chern-simons term, *Progress of Theoretical Physics Supplement* **123**, 61 (1996).